International Journal of Modern Chemistry, 2018, 10(2): 233-255

Modern Scientific Press

International Journal of Modern Chemistry **ISSN: 2165-0128**

Journal homepage: www.ModernScientificPress.com/Journals/IJMChem.aspx *Florida, USA*

Article

Electrochemical Study for Effect of Gliclazide as a Corrosion Inhibitor of the Carbon Steel in Sulfuric Acid Medium by Applied Potentiondynamic and Evans Techniques

Adel H. Ali

Department of medicinal chemistry, Faculty of medical Science, Taiz University, Yemen

E-Mail: Adelchemst22@gmail.com

Article history: Received 5 July 2018, Revised 30 August 2018, Accepted 6 September 2018, Published 20 September 2018.

Abstract: This paper is to study a possibility of using pharmaceutical drug compound like N-(hexahydrocyclopenta[c]pyrrol-2(1H)-ylcarbamoyl)-4-methylbenzenesulfonamide as corrosion inhibitor that can have a decisive effect of decreasing on metallic corrosion rate and adsorbed on the metal surface by using potentiodynamic polarization and Evans techniques. In this regard, we simultaneously present an overview on gliclazide compound performance, as corrosion inhibitor in 10% ethanol, 0.5N H_2SO_4, in mixed solution (10 % ethanol, 0.5N H_2SO_4) and the mixed solution with presence different concentration of drug. The potentiodynamic polarization and Evans technique are studied the C-steel in different medium to clarify the effect of media on the corrosion processes, the effect of polarization on the orientation of inhibitor molecule and discussed the mechanism of the adsorption processes on the polarized metal surface, i.e. the inhibition cathodicaly or anodicaly.

Keywords: corrosion inhibition; potentiodynamic polarization; Evans technique; mixed solution; gliclazide inhibitor.

1. Introduction

Most organic compounds containing nitrogen (N-heterocyclic), sulfur, long carbon chain or aromatic and oxygen atoms. Among them, organic compounds have many advantages such as: high

molecular size, highly soluble in water, availability, cheap, low toxicity, easy for using and easy production **[1]**. Natural heterocyclic mixes have been utilized for the corrosion inhibitor on the C-steel **[2]**, copper **[3]**, aluminum **[4]**, and various metals in various aqueous medium **[5]**. Adsorption of the drug molecules on the metal surface facilitates its inhibition **[6]**. The investigation of the relations between the adsorption and consumption hindrance is of awesome important. Heterocyclic mixes have demonstrated more hindrance effectiveness for C-steel in both HCl **[7]** and H_2SO_4 arrangements **[8]**.

2. Experimental

2.1. Metal Samples

Two samples of carbon steel was used in the study that have the chemical composition of the metal samples was determined using emission spectrometer, with the aid of ARL quant meter (model 3100-292 IC) and listed in the **Table 1**.

Table 1: Chemical compositions of carbon steel sample

Sample	C%	Mn%	V%	Fe%	Si%
Low; C	0.26	0.77	0.11	98.51	0.35

2.2. Preparation of Metal Sample (Working Electrode)

The working electrode having the surface area, which, exposed to corrosion media are ($1.321Cm^2$) and every rod was weld from one side to a copper wire used for electric connection. The sample was embedded in glass of just larger diameter than the sample. Epoxy resin was used to stick the sample to glass tube. These also insured that constant cross-sectional area would be exposed to corrosive media through the experiments. The exposed area was grinded with different apperceive papers in the normal way, initially with course grade and gradually to finer grade, then finally with the finest grade. Then the polishing using alumina paste on as mentioned before. Finally polishing of sample surface to be mirror bright, followed by washing with distilled water then with acetone and finally with doubly distilled water, just before immersion in the electrolyte cell.

2.3. Gliclazide Drug as an Inhibitor

The gliclazide (**$C_{15}H_{21}N_3O_3S$**) inhibitor have molecular mass (323.412 g/mol), (3O) oxygen atoms, (3N) nitrogen, (S) sulfur and benzene range.

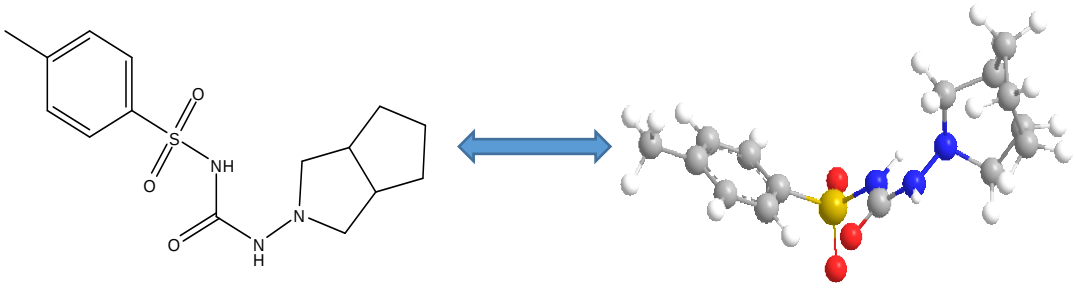

N-(hexahydrocyclopenta[c]pyrrol-2(1H)-ylcarbamoyl)-4-methylbenzenesulfonamide

2.4. Solutions

a) All solutions were prepared from analytical grade chemical reagents and used without further purification. Different concentration of H_2SO_4 (0.1, 0.5 and 1N) were prepared and standardized by NaOH (where NaOH standardized against KH-phthalate), this concentrations were prepared in different concentration of ethanol (10%, 20% and 30%). Then used as corrosion media.

b) A stock solution of gliclazide was prepared by dissolving 0.016 gm gliclazide in one liter [0.5N H_2SO_4 in 10% ethanol-water] to obtain 10^{-4} M gliclazide solution. This stock solution then diluted by [0.5N H_2SO_4 in 10% ethanol-water] to prepare desired other solution. These solutions were used as corrosion medium.

All solution was prepared from analytical grade chemical reagent, which was used 0.5N of H_2SO_4 mixed with 10%ethanol. This mixed solution used corrosive media and add the different of concentrations of gliclazide (2×10^{-5}, 4×10^{-5}, 6×10^{-5}, 8×10^{-5} and 10×10^{-5} molar) to the corrosive media at different temperatures (15, 25, 35, 45 and 55^{o}C).

2.5. Potentiodynamic Polarization Measurement [9,10]

Cathodic and anodic polarization technique was used for determination of corrosion rate. The electrochemical cell consists of three electrodes:

(i) Platinum electrode (as an auxiliary electrode).

(ii) Calomel electrode (as the reference electrode). It was a saturated calomel electrode (SCE) prepared from very pure chemicals. The calomel past was shaken with repeated changes of saturated KCl before it was introduce in the container over the pure mercury. Over the surface of the calomel past, there were always crystals of KCl was presented over the surface of calomel past, in order to ensure saturation solution. This electrode was written as follow:

$$(Hg_{(l)} \mid Hg_2Cl_{2(s)}, KCl_{(aq)}sat,)\ E= -\ 241\ mV\ at\ 25^oC.$$

(iii) The working electrode is C-steel sample. The electrolytic cell was filled with 100 ml of the solution. The samples were immersed in the medium, then the circuit is shorted and the cathodic polarization is firstly measured by reverse the current direction the anodic polarization is measured.

2.6. Calculation of Rate of Corrosion

The anodic and cathodic polarization is measured by using over-potential cell. The corrosion current density (I_{corr}), the corrosion potential (E_{corr}) and the corrosion rates (R) are calculated according to Tafel extrapolation method **[11]**.

It is clear that extrapolating the line representing the Tafel region in either cathodic or anodic polarization curve to the corrosion potential will give corrosion current density (I_{corr}), which can be used to calculate the corrosion rate from the equation **[12, 13]**.

Corrosion rate (mpy) = 0.1288 I_{corr} (mA/cm2) Eq.wt /d (g/cm3)

Where, Corrosion rate (mpy) = mils per year,
I_{corr} = the corrosion current density,
d = Specimen density, and,
Eq.wt = Specimen equivalent weight.

The corrosion current density (I_{corr}), corrosion potential (E_{corr}) and corrosion rate are recorded in **Table 7**.

2.7. Applied Evans Technique

The rate of corrosion can be understood from a graphical superposition of current-potential curves. The Evans diagrams give good and suitable interpretation about the electrode-electrolyte interface reactions. We can use the following definitions for the items of Evans diagram as follows **[14]**:

(i) $\Delta\phi_{e,m}$ and $\Delta\phi_{e,so}$ are anodic and cathodic potentials at equilibrium at the electrode-electrolyte interface (at I =the exchange current i_o) respectively, where $\Delta\phi e,x = E_{e,x} \pm \left| E_c - E_a \right| i=i_o$; m= metal, so= solution,

(ii) $\Delta\phi = \Delta\phi_{corr}$ = the relative corrosion potential determined from the position of the intersection of the two curves (de-electronation and electronation processes) where, I considered as i_{corr}.

(iii) The anodic- potential difference at equilibrium (a.p.d,e) $\Delta\phi'_m = \eta_m = \Delta\phi_{corr} - \Delta\phi_{e,m}$.

(iv) The cathodic- potential difference at equilibrium (c.p.d,e) $\Delta\phi'_s = \eta_{so} = \Delta\phi_{corr} - \Delta\phi_{e,so}$.

(v) The anodic-potential difference (a.p.d) $\Delta\phi'_a = (\Delta\phi_a)_x - (\Delta\phi)_b$; b =bulk, x = with additive, at different concentrations or at different temperatures, and $\Delta I_a = (i)_b - (I)_x$.

(vi) The cathodic-potential difference (c.p.d) $\Delta\phi'_c = (\Delta\phi)_b - (\Delta\phi_c)_x$; b=bulk, x= with additive, at different concentrations or at different temperatures, and $\Delta I_c = (i)_b - (I_c)_x$.

These data can be used for kinetic calculations and to know which additive is favorable or which is faster to the electrode surface at the same conditions. It can be used for studying the inhibition mechanism and aids in the classification the additives.

3. Result and Discussion

3.1. Potentiodynamic Polarization Technique

Study the polarization of the deferent medium and with added the various concentration of gliclazide as a corrosion inhibitor.

3.1.1. Dissolution of steel sample in 0.5N H_2SO_4 at different temperatures

Results of the anodic and cathodic polarization processes for the two C-steel (LCA) sample in 0.5N H_2SO_4 at different temperatures in absence of gliclazide are shown in **Figure 2** and **Table 2**. It obvious that the corrosion current density (I_{corr}) is increased as the temperature increased and the corrosion potential (E_{corr}) is slightly shafted to more value that is positive. The polarization processes are started with potential between of about 530 and 550 which, lays in the first passivity region of theoretical iron corrosion diagram (from Pourbaix atlas E-PH diagram **Figure 1**) **[15]** front of **pH = 0.3 (area A).** It is obvious that refer to steady state potential where the rate of corrosion is equilibrium with thin film formation. The positive potential is increased by anodic polarization, i.e. increase the dissolved component while that the potential decreased by cathodic polarization, i.e, increase the undissolved components. The dissolved component is formed as:

$$Fe \rightarrow Fe^{2+} + 2e$$

$$Fe^{2+} + 2H_2O \rightarrow HFeO^-_2 + 3H^+$$

Where, $HFeO^-_2$ Di-hypo-ferrite, green.

In the same time occurs as: $HFeO_2^- + H^+ \rightarrow Fe(OH)_2$

Where, the undissolved hydrated and the (Fe O) can be considered. So that at anodic polarization in presence of H_2SO_4, the iron is dissolved and formed ferrous sulphate as:

$$Fe^{2+} + H_2SO_{4(aq)} \rightarrow Fe\,SO_{4(aq)} + 2H^+$$

And the cathodic processes in presence of H_2SO_4, occurred as:

i) $2H^+ + 2e \rightarrow H_2$ hydrogen evolution

ii) $O_{2(g)} + 4H^+_{(aq)} + 4e \rightarrow 2H_2O_{(l)}$ reduced of oxygen

The hydrogen ions adsorbed on the metal surface where an electro chemical reaction takes place in presence of O_2 as;

$$M + H_3O^+ + e \rightarrow M{-}H + H_2O$$

Where three steps can be done as;

a) $2M{-}H \rightarrow 2M + H_{2(g)}\uparrow$

b) $M{-}H + H_3O^+ + e \rightarrow M + H_{2(g)}\uparrow + H_2O$ or

c) $4M{-}H^+ + \text{dissolved } O_2 + 4e \rightarrow 4M + 2H_2O_{(l)}$

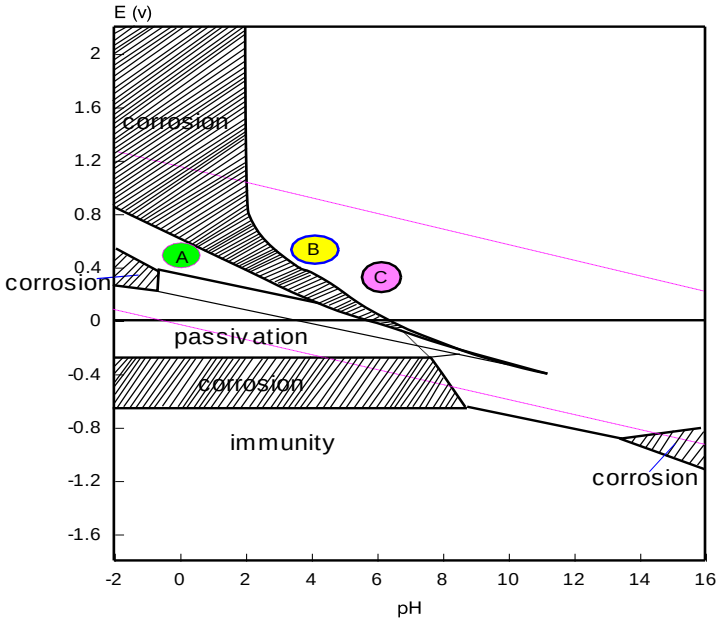

Figure 1: E-PH diagram of steel corrosion

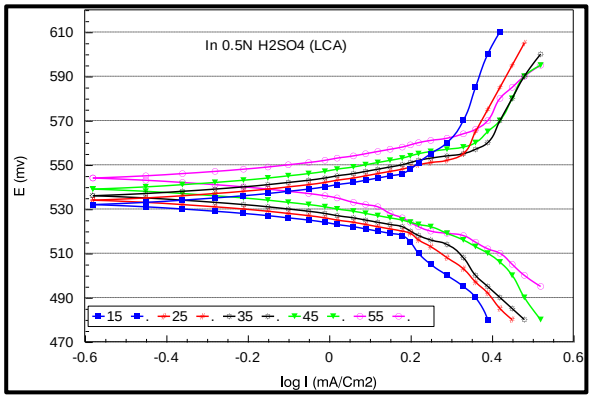

Figure 2: The potentiodynamic polarization curves for the corrosion of C-steel (LCA) in 0.5 N of H_2SO_4.

3.1.2. Dissolution of steel samples in 10% ethanol at different temperatures

Results of the anodic and cathodic polarization processes for the two C-steels samples (LCA) in 10 % ethanol at different temperatures in absence of gliclazide is shown in **Figure 3** and **Table 2**. It obvious that the corrosion current density (I_{corr}) is increased as the temperature increased and the

corrosion potential (E_{corr}) is shafted to value that is more positive.

The polarization processes are started with potential between of about 270 and 430 mV which, lays in the second passivity region of theoretical iron corrosion diagram (from Pourbaix atlas E-PH diagram **Figure 1**) front of **pH= 6.8 (area C).** It is obvious that refer to steady state potential where the rate of corrosion is equilibrium with thin film formations. The positive potential is increased by anodic polarization, i.e. increase the dissolved component while that the potential decreased by cathodic polarization, i.e., increase the undissolved components. The dissolved component is formed during the polarization reaction of steel in the presence of 10 % ethanol as:

$$Fe \rightarrow Fe^{2+} + 2e \quad \text{anodic reaction}$$

$$2H_2O + 2e \rightarrow H_{2\,(g)} \uparrow + 2OH^- \quad \text{cathodic reaction}$$

In total process:

$$Fe + H_2O \rightarrow Fe^{2+} + 2OH^- \rightarrow Fe(OH)_2$$

In the bulk the ferrous hydroxide dissolved as:

$$2Fe(OH)_2 \rightarrow 2FeOH^{++} + 2OH^-$$

And, $2Fe\,OH^{++} + 2e \rightarrow 2Fe\,O + H_2\uparrow$

Where, the undissolved hydrated and the (Fe O) can be considered at area C too.

Table 2: The corrosion potential, corrosion current density and rate of corrosion for (LCA) in 10 % ethanol and 0.5N H_2SO_4 at different temperatures.

Concentration	Temp.	E_{corr}(mV)	I_{Corr}(mA/Cm^2)	Rate (mpy)
10% Ethanol	288K	320	0.06	0.027
	298K	340	0.07	0.033
	308K	370	0.09	0.041
	318K	400	0.10	0.047
	328K	430	0.14	0.065
0.5 N H_2SO_4	288K	532	1.32	0.60
	298K	534	1.43	0.65
	308K	536	1.55	0.71
	318K	539	1.66	0.76
	328K	544	1.82	0.83

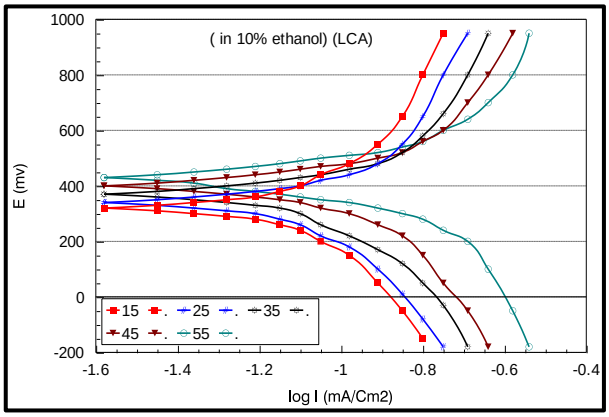

Figure 3 : The potentiodynamic polarization curves for the corrosion of C-steel (LCA) in 10% of ethanol.

3.1.3. Dissolution of steel in mixed (0.5N H_2SO_4 +10%Ethanol)

Results of the anodic and cathodic polarization processes for the C-steels sample (LCA) in mixed solution at different temperatures in absence of gliclazide is shown in **Figure 4** and **Table 7**. It obvious that the corrosion current density (I_{corr}) is increased as the temperature increased and the corrosion potential (E_{corr}) is shafted to the value that is more positive.

The polarization processes are started with potential between of about 520 and 530 mV which, lays in the second passivity region of theoretical iron corrosion diagram (from Pourbaix atlas E-PH diagram **Figure 1**) front of **pH = 4.8 (area B)**. It is obvious that it has the same steady state behavior. The positive potential is increased by anodic polarization, i.e. increase the dissolved component while that the potential decreased by cathodic polarization, i.e, increase the undissolved components. The corrosion and passivity processes as discussed before. The results at 25^o C from **Figure 5** and the comparison of I_{corr} in those three media are listed in **Table 3**.

Table 3: Comparison between three medium

Corrosive medium	Current density (I_{corr})
	LCA
10% Ethanol	0.071
0.5 N H_2SO_4	2.429
Mixed	2.161

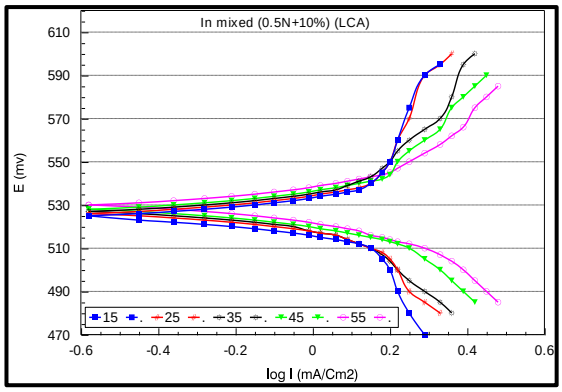

Figure 4 : The potentiodynamic polarization curves for the corrosion of C-steel (LCA) in mixed [10 % ethanol and 0.5 N H_2SO_4] in the nonexistence of varied concentration of gliclazide at various temperatures.

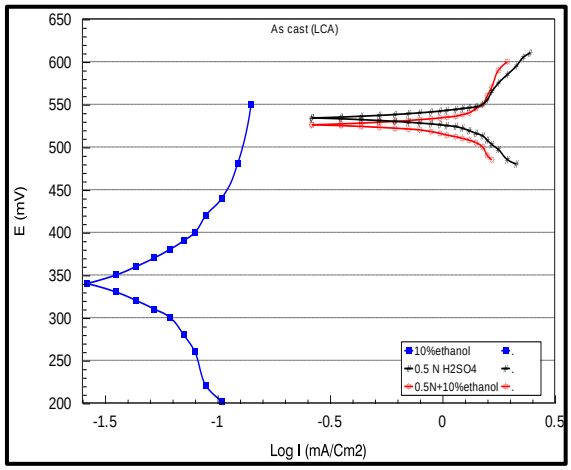

Figure 5: The comparison between the polarization effects in the three mediums at 25°C (As cast LCA).

These results concluded that:

(i) the corrosion rate in 0.5N H_2SO_4 is very high where the major product is the dissolved component $FeSO_4$ while the formation of undissolved component FeO is very low and slightly detected, where I_{corr} is rise too (2.429)

(ii) In the second passivity region (in presence of 10% ethanol), the undissolved component is considered where the I_{corr} is dropped to (0.071).

(iii) In the presence of mixed medium, the corrosion rate still very high where I_{corr} is listed (2.161) and the undissolved component can be slightly considered.

3.1.3.1. Effect of 10% ethanol on the corrosion of steel in 0.5N H_2SO_4 at different temperature

Result of the anodic and cathodic polarization of C-steel in 0.5N H_2SO_4 with 10 % ethanol at different temperatures (15, 25, 35, 45 and 55°C) are shown in **Figure 4**.

a) Ptentiodynamic polarization technique

In general, as the added 10% ethanol is shifted the potentials to less positive values comparing with only 0.5N H_2SO_4 and both anodic potential E_a and cathodic potential E_c are shifted to less positive values. The anodic current (i_a) slightly decreased (shifted to less values) while the cathodic (i_c) decreased and shifted to less values too, **Figures 6** at different temperatures.

Values of corrosion potential (E_{corr}), corrosion current density (I_{corr}) and rate of corrosion in (mpy), are given in **Table 7**.

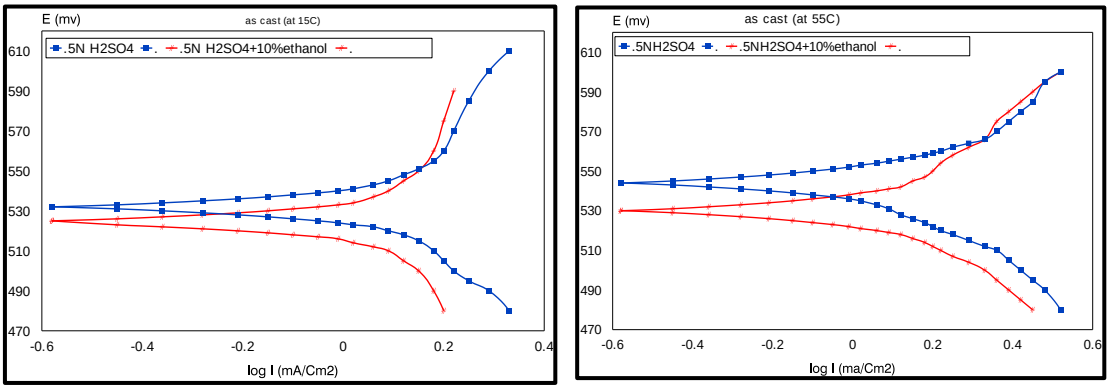

Figure 6: Effect of add 10% ethanol to 0.5N H_2SO_4 on anodic and cathodic polarization curves of LCA metal at different temperatures.

b) Applied Evans technique

Applying the principle of Evans diagrams in presence of 10%ethanol with 0.5N H_2SO_4, was drown in **Figures 7** and the Evans diagram parameters was recorded in the **Table 4**, it is clear that:

The relative corrosion potential ($\Delta\phi_{corr}$) shifted slightly to values that are more positive. The relative corrosion current (i_{corr}) increases with temperatures increasing.

The potential difference ($\Delta\phi'_m$) is slightly increased with temperature increased and the ($\Delta\phi'_s$) is increased to high values too. The transference coefficient of cathode (α_c) is increased with temperature increasing but the transference coefficient of anode (α_a) is decreased with increasing of temperatures.

The anodic-potential difference $|\Delta\phi'_a|$ is increased by temperature increased and the cathodic-potential difference $|\Delta\phi'_c|$ is increased slightly by temperature increased. The differences in anodic corrosion current $|\Delta I_a|$ and cathodic corrosion current $|\Delta I_c|$ are slightly increased by temperature increased. The values of ratio ($\Delta\phi'_a/\Delta I_a$) are decreased by temperature increased and the ratio of ($\Delta\phi'_c/\Delta I_c$) are increased by temperature increased.

From the results illustrated in Evans diagrams for the electrode - electrolyte interface in (LCA) it is clear that:

The presence of 10 % ethanol under polarization technique shifted the de-electronation potential toward more positive values (positive direction), this means that the polarization oriented and collective the ethanol molecules to the electron sink site on the electrode surface and slow down the metal dissolution. Moreover, the presence of 10 % ethanol under polarization technique shifted the electronation potential of acceptor spices to less positive values (negative directions), this means that the collective ethanol molecules are not only adsorbed on the electron sink area, but also the collective ethanol molecules covered the electron source area too. It is clear that, it slowing down (more and more) both the metal dissolution and the hydrogen evolution.

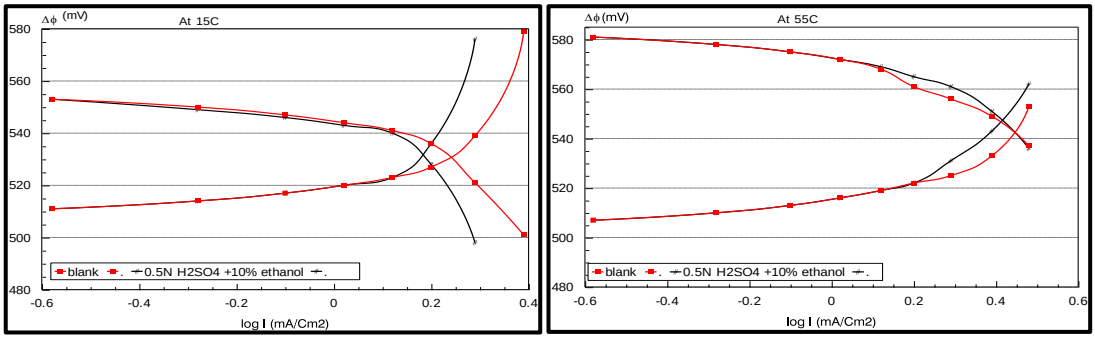

Figure 7: Evans diagrams of electronation and de-electronation potentials versus log I for LCA in (10A5H) at different temperatures.

Table 4: Relative parameters from Evans diagram of LCA in mixed solutions (10A5H).

Temp.	Δφcorr	Icorr	Δφe,m	Δφe,so	Δφ'm	Δφ's	(i)b	(Δφ)b	(Δφ'a)x	Δφ'a	(ΔIa)x	ΔIa*	Δφ'a/ΔI	(Δφ'c)x	Δφ'c	(ΔIc)x	ΔIc	Δφ'c/ΔI	α,a	α,c
288	531.5	1.44	511	553	20.5	21.5	1.738	530.5	527	-3.5	1.59	0.2	-22.9	536	-5.5	1.6	0.14	-40.7	0.49	0.51
298	535	1.55	513	555	22	20	1.906	530	539.5	9.5	1.64	0.3	35.85	529	1	1.7	0.21	4.808	0.52	0.48
308	536	1.71	509	563	27	27	2.239	530	543	13	1.86	0.4	34.48	527	3	1.95	0.29	10.38	0.5	0.5
318	544	1.97	511	567	33	23	2.483	537	546	9	2.02	0.5	19.35	533	4	2.32	0.17	24.1	0.59	0.41
328	547	2.63	507	581	40	34	2.818	543	546	3	2.6	0.2	13.76	542	1	2.79	0.03	31.25	0.54	0.46

3.1.3.2. Effect of add different concentration of gliclazide inhibitor

Result of the anodic and cathodic polarization of C-steel in mixed solution (10A5H) with different

concentrations of gliclazide (2, 4, 6, 8 and $10x10^{-5}$ M) at 25°C are shown in **Figure 8**.

a) Potentiodynamic polarization technique

It is obvious that the presence of different concentrations are shifted the potentials to less positive values and both anodic potential E_a and cathodic potential E_c are shifted to less positive values. The anodic current (i_a) slightly decreased (shifted to less values) while the cathodic (i_c) decreased and shifted to less values too shown in **Figure 9**.

Values of corrosion potential (E_{corr}), corrosion current density (I_{corr}) and rate of corrosion in (mpy), are given in **Table 7**.

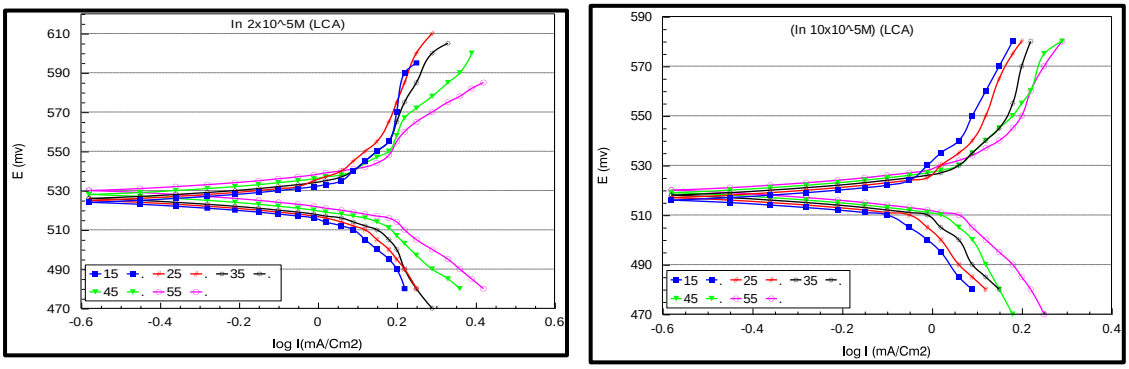

Figure 8 : The potentiodynamic polarization curves for the corrosion of C-steel in (10% ethanol and 5N H_2SO_4) with existence low and high concentration of gliclazide at various temperatures.

b) Applying Evans technique

Applying the principle of Evans diagrams in presence of different concentrations from gliclazide, which are viewed in **Figures 10**, and the Evans diagram parameters are listed in **Table 5**, it is clear that:

The relative corrosion potential ($\Delta\phi_{corr}$) shifted slightly to less positive values. The relative corrosion current (i_{corr}) decreases with temperatures increasing.

The potential difference ($\Delta\phi'_m$) is decreased with temperature increased and the potential difference ($\Delta\phi'_s$) is increased to high values with increasing of temperatures. The transference coefficient of cathode (α_c) is increased with temperature increasing but the transference coefficient of anode (α_a) is decreased with increasing of temperatures.

The anodic-potential difference $|\Delta\phi'_a|$ is not affect by temperature increased and the cathodic-potential difference $|\Delta\phi'_c|$ is increased by temperature increased. The differences in anodic corrosion current $|\Delta I_a|$ are not affects and cathodic corrosion current $|\Delta I_c|$ are increased by temperature increased. The values of ratio ($\Delta\phi'_a/\Delta I_a$) are decreased by temperature increased and the ratio of ($\Delta\phi'_c/\Delta I_c$) are decreased by temperature increased.

From the results illustrated in Evans diagrams for the electrode- electrolyte interface in (LCA), it

is clear that:

In presence concentrations of gliclazide under polarization technique, at low gliclazide concentrations the de-electronation potential shifted toward more positive values (positive direction) this means that the polarization affected the donor functional groups of gliclazide molecules and oriented them to the electron sink area on the electrode surface and slow done the dissolution of metal. The moderate size of gliclazide molecules allow to cover somewhat area of electron source, so that the electronation potential of acceptor spices to less positive value. It is observed that the shifted of de-electronation potential is larger than the shift of electronation potential. As the gliclazide concentration increased the shift of electronation potential i.e., the gliclazide molecules covered more electron source area on the corroded metal surface with increasing gliclazide concentration and the electronation potential shift is being larger than the de-electronation potential shift, which indicates slightly formation of multilayer that adsorbed on the electrode surface. It is clear that the polarization process affects the orientation and adsorption of the inhibitor molecules, so that both the metal dissolution and the hydrogen evolution is slowing down more and more.

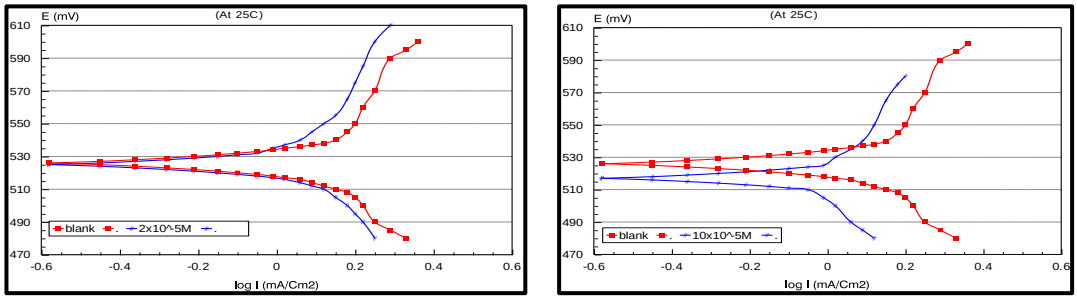

Figure 9: Effect of add different concentration of gliclazideon anodic and cathodic polarization curves of LCA metal at constant temperature (25^{o}C).

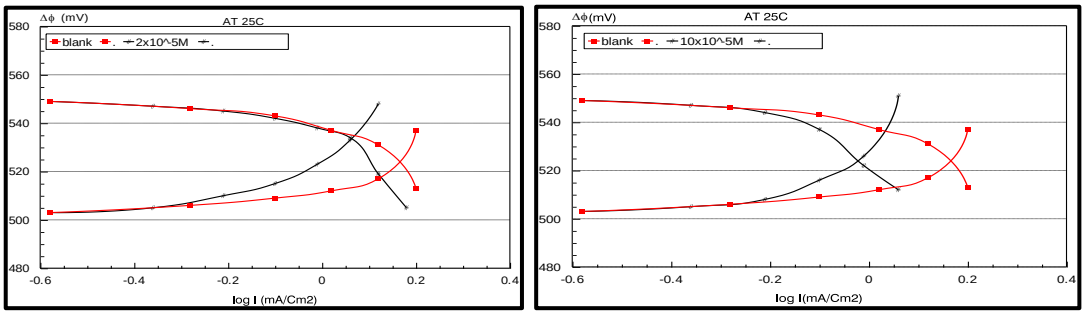

Figure 10: Evans diagrams of electronation and de-electronation potentials versus log I for LCA with different concentration of gliclazide at 25^{o}C.

Table 5: Relative parameters from Evans diagram of LCA with different concentration of gliclazide at 25°C.

Temp.	Δφcorr	Icorr	Δφe,m	Δφe,so	Δφ'm	Δφ's	(i)b	(Δφ)b	(Δφ'a)	Δφ'a	(ΔIa)x	ΔIa*	Δφ/ΔI,	(Δφ'c)x	Δφ'c	(ΔIc)x	ΔIc	Δφ'/ΔI,	α,a	α,c
288	534	1.2	503	549	31	15	1.5	524	535	11	1.2	0.3	37.2	518	6	1.35	0.13	46.2	0.7	0.3
298	532	1.1	503	549	29	17	1.5	524	535	11	1.2	0.3	35.6	517	7	1.3	0.2	43.5	0.6	0.4
308	530	1.1	503	549	27	19	1.5	524	535	11	1.16	0.3	34.6	516	8	1.3	0.2	41.9	0.6	0.4
318	527	1.1	503	549	24	22	1.5	524	535	11	1.1	0.4	30.8	514	10	1.2	0.3	32.9	0.5	0.5
328	524	0.4	503	549	21	25	1.5	524	536	12	1.1	0.4	30.4	513	11	1.1	0.4	30.8	0.5	0.5

3.1.3.3. Effect of temperature on corrosion behavior

Results of the anodic and cathodic polarization processes for the C-steels samples (LCA) in various media, The E_{corr}, I_{corr} and the rate of corrosion were increased with temperatures increased at the same concentration of gliclazide, which are listed in **Table 7** and **Figures 11**.

a) Potentiodynamic polarization technique

This behavior indicating to the corrosion rate of steel stimulates with increasing of temperature and increasing of temperatures will be enhance the rate of diffusion of hydrogen (H^+) ion to the metal surface beside the ionic mobility, thus increasing the conductivity of the electrolyte. Also, at lower temperatures, absorbed hydrogen atoms which are blocked on the cathodic areas, otherwise the increasing of the solution temperature, hydrogen will be disrobed, from the cathodic area, i.e the corrosion rate increased.

b) Apply Evans technique

Applying the principle of Evans diagrams in presence of $4x10^{-5}$M from gliclazide, which are viewed in **Figures 12** and the Evans diagram parameters are listed in **Table 6**, it is clear that:

The relative corrosion potential ($\Delta\phi_{corr}$) shifted slightly to values that are more positive. The relative corrosion current (i_{corr}) is increases with temperatures increasing.

The potential difference ($\Delta\phi'_m$) is slightly increased with temperature increased and the potential difference ($\Delta\phi'_s$) is increased to high values with increasing of temperatures. The transference coefficient of cathode (α_c) is increased with temperature increasing but the transference coefficient of anode (α_a) is decreased with increasing of temperatures.

The anodic-potential difference $|\Delta\phi'_a|$ is decreased by temperature increased and the cathodic-

potential difference $|\Delta\phi'_c|$ is slightly decreased by temperature increased. The differences in anodic corrosion current $|\Delta I_a|$ are not affects and cathodic corrosion current $|\Delta I_c|$ are slightly decreased by temperature increased. The values of ratio $(\Delta\phi'_a/\Delta I_a)$ are decreased by temperature increased and the ratio of $(\Delta\phi'_c/\Delta I_c)$ are decreased by temperature increased.

From the results illustrated in Evans, diagrams for the electrode- electrolyte interface it is clear that:

The effect of temperature on the behavior of gliclazide as inhibitor of steel corrosion, at $4x10^{-5}$M gliclazide was chosen. It observed that:

1) At low temperature (15°C), the de-electronation and electronation potential are equal.

2) By increasing the temperature, the de-electronatin potential shifted to more positive value, on the other hand the electronaion potential unaffected.

This observation clarifies that the adsorption of gliclazide on electron sink area has physical-chemical adsorption properties on LCA surface.

From the results illustrated in Evans, diagrams for the electrode- electrolyte interface it is clear that:

The effect of temperature on the behavior of gliclazide as inhibitor of steel corrosion, at $4x10^{-5}$M gliclazide was chosen. It observed that both electronation and de-electronation potentials are shifted to negative and positive direction respectively by increasing the temperature. This behavior clarify that the heat treatment divided the electron sink and electron source area to small parts, so that the size of gliclazidesufficient to cover more electron source area be side electron sink.

Table 6: Relative parameters from Evans diagram of LCA in presence of $4x10^{-5}$M of gliclazide at different temperatures.

Temp.	Δφcorr	Icorr	Δφc,m	Δφc,so	Δφ'm	Δφ's	(i)b	(Δφ)b	(Δφ'a)x	Δφ'a	(ΔIa)x	ΔIa*	Δφ/ΔI,a	(Δφ'c)x	Δφ'c	(ΔIc)x	ΔIc	Δφ'/ΔI,c	α,a	α,c
288	530	1.4	509	549	21	19	1.5	527	532	5	1.4	0.1	49.5	525	2	1.5	0.03	57.14	0.53	0.5
298	531	1.5	510	552	21	21	1.7	531	534	3	1.5	0.1	21.9	525	6	1.5	0.2	41	0.5	0.5
308	532	1.6	509	555	23	23	1.9	530	535	5	1.7	0.1	34.7	527	3	1.7	0.1	23	0.5	0.5
318	533	1.9	509	557	24	24	2.0	530	534	3.5	1.9	0.1	23.8	528	2.5	1.9	0.1	22	0.5	0.5
328	529	2.2	506	564	23	35	2.5	532	534	2	2.4	0.1	17.7	528	4	2.24	0.27	14.6	0.4	0.6

Table 7: The effect of (gliclazide) additions on the E_{corr}, I_{corr} and rate of corrosion for (LCA) in (10A5H) at different temperatures

Conc.[I]x 10^5M	Temp. K	E_{corr} (mV)	I_{corr} (mA/Cm^2)	Rate (mpy)	Θ	% IE
0.00	288	530	2.122	1.96	----	----
	298	531	2.161	1.99	----	----
	308	532	2.216	2.05	----	----
	318	533	2.318	2.15	----	----
	328	535	2.514	2.33	----	----
2.00	288	529	1.25	1.16	0.411	41.1
	298	530	1.294	1.20	0.401	40.1
	308	531	1.351	1.25	0.390	39.0
	318	533	1.423	1.32	0.386	38.6
	328	535	1.535	1.42	0.389	38.9
4.00	288	527	1.208	1.12	0.431	43.1
	298	528	1.25	1.16	0.422	42.2
	308	529	1.332	1.23	0.399	39.9
	318	530	1.381	1.28	0.404	40.4
	328	531	1.477	1.37	0.412	41.2
6.00	288	525	1.176	1.09	0.446	44.6
	298	526	1.224	1.13	0.434	43.4
	308	527	1.294	1.20	0.416	41.6
	318	528	1.351	1.25	0.417	41.7
	328	529	1.402	1.30	0.442	44.2
8.00	288	523	1.146	1.06	0.460	46.0
	298	524	1.199	1.11	0.445	44.5
	308	525	1.259	1.16	0.432	43.2
	318	526	1.313	1.22	0.434	43.4
	328	527	1.361	1.26	0.458	45.8
10.00	288	521	1.131	1.05	0.467	46.7
	298	522	1.161	1.07	0.463	46.3
	308	523	1.208	1.12	0.455	45.5
	318	524	1.267	1.17	0.453	45.3
	328	525	1.341	1.24	0.467	46.7

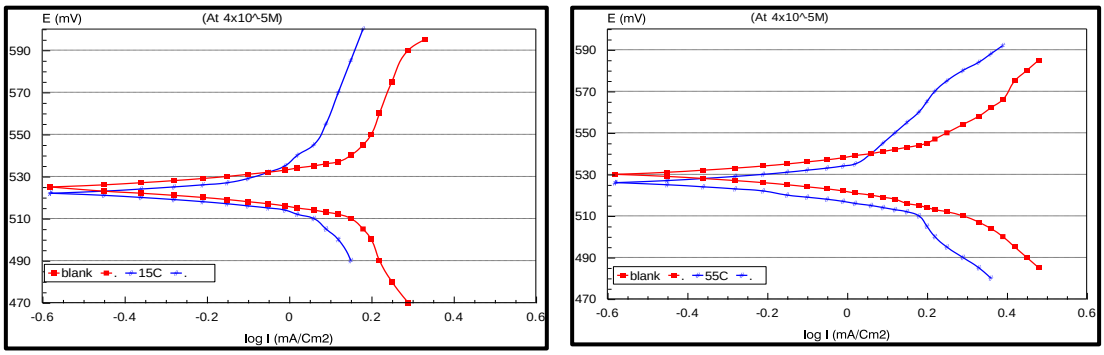

Figure 11: Effect of temperatures in presence $4x10^{-5}$M of gliclazide on anodic and cathodic polarization curves of LCA metal.

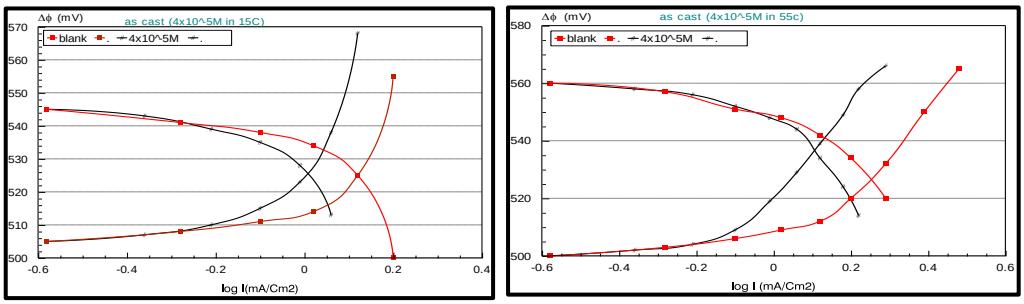

Figure 12: Evans diagrams of electronation and de-electronation potentials versus log I for LCA in presence of $4x10^{-5}$M of gliclazide at different temperatures.

3.2. Inhibition Efficiency (IE %)

The gliclazide compound has eight active centers as; 3O, 3N, S atoms and benzene rang all act as donor center. Because of the restricted un-plainer structure of gliclazide, not all active group acts in the same time. These centers oriented to anodic sites (iron carbide) and adsorbed on it. The gliclazide molecule attached with anodic site and covered somewhat of cathodic area, so that the corrosion rate in presence of gliclazide is anodic-cathodic control. The inhibition efficiency (IE %) is calculated as following **[16]**.

$$IE\ \% = [(I_{corr} - I'_{corr})/I_{corr}] \times 100 \qquad (1)$$

Where; I_{corr} and I_{corr}' are the corrosion current density in absence and presence of inhibitor respectively. The inhibition efficiency data in **Table 7**, obvious that this inhibition efficiency for carbon steel sample under study increases with increasing gliclazide concentration in the following order:10^{-4}>$8x10^{-5}$>$6x10^{-5}$>$4x10^{-5}$>$2x10^{-5}$ M of gliclazide drug

Plot IE % against logarithm of gliclazide inhibitor concentrations (log [I]), obvious that in cases 288, 298, 308 and 318^{o}K, the inhibition efficiency (IE %) decreased as the temperature of the medium is increased, but the (IE %) in 318^{o}K increased, this behavior indicated that chemisorptions occurs. See

Figure 13. The extra part in the curvatures that obtained from polarization technique than S shape indicates that there are multilayer proceed from the orientation of functional group under polarization where caused second chemical adsorption over the first layer **[17]**.

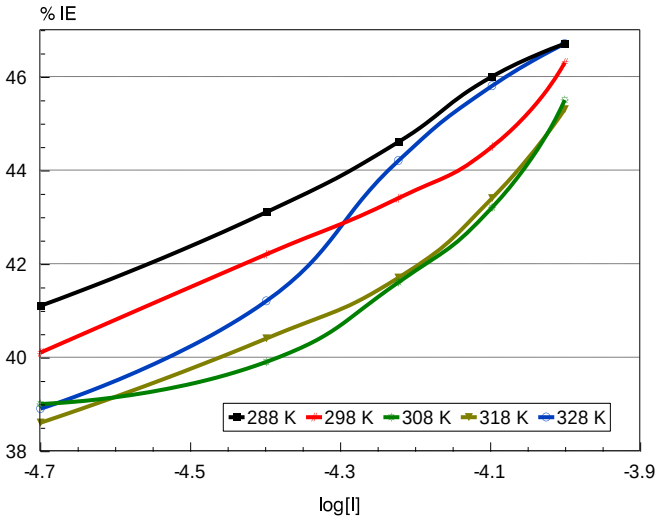

Figure 13: The relation between inhibition efficiency and log [I] in [mixed 10% ethanol and 0.5 N H_2SO_4] for (LCA) at various temperatures.

3.2.1. Mechanism of inhibition

To illustrate the mechanism of inhibition of corrosion on the C – steel surface in acid medium by using pharmaceutical drug compound as an inhibitor, it is must be know the nature of metal surface and the nature of the component of inhibitor structure. The C – steel is regarded the metal α-phase **[18]**, It is obvious that α-phase state consists of grains and grain boundaries in the surface of the metal, **Figure 14**. A cross-section of a piece or specimen of the metal that is a corroding to clarify that there are both anodic and cathodic sites in the metal surface structure.

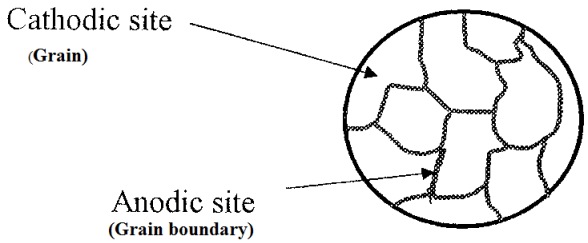

Figure 14: Schema models of metalα- phase

The surface of iron is usually, coated with a thin film of iron oxide **[11]**. However, if this iron oxide film develops some cracks, anodic area are created on the surface, while other metal parts act as cathodes. It follows that the anodic areas are small surface, while nearly the rest of the surface of the

metal large cathodes.

Electrochemical corrosion involves flow of electric current between the anodic and cathodic areas called inter-granular corrosion **Figure 15**. SEM image is shown the corrosion of C – steel in 0.5 N H_2SO_4in one day immersion that illustrated inter-granular corrosion.

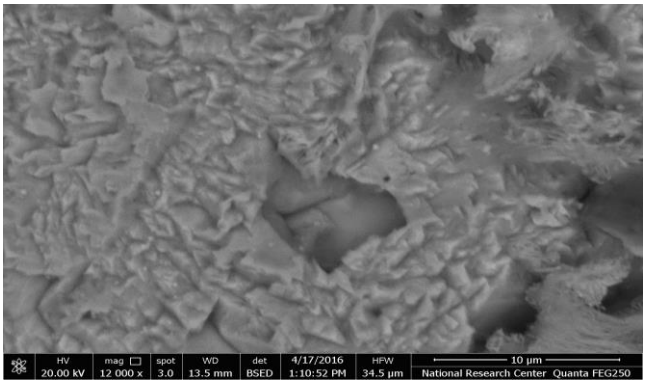

Figure 15: SEM image illustrated inter-granular corrosion after immersion the specimen in 0.5N H_2SO_4one day

All previous results prove that the pharmaceutical drug compound under study were actually inhibit the corrosion of C – steel in H_2SO_4 acid solution as a corrosive medium. The corrosion inhibition is due to their physical adsorption and formation of protection thin film adsorbed on the metal surface. The effect of pharmaceutical drug compound under study as inhibitor may be corresponding to the accumulation of the inhibitor molecules on the metal surface, which prevent the direction contact of the metal surface with corrosive environment. The surface of the C – steel sample is positively charge in aqueous acid solution **[19, 20]**. The partial negative charge that present in function group (O, S and N) and electronic density of benzene ring in pharmaceutical drug molecules under study may be adsorbed on the positively charge of the metal surface like electrostatic attraction between the opposite charge, in the form of neutral molecules, that involving displacement of water molecules from the metal surface and sharing electrons between π bonding electron density and unshared electrons of oxygen and nitrogen to the metal surface **[21]**, **Figure 16**. The inhibition action of the inhibitor can be accounted by the interaction between the lone pair of electrons in the O, S and N atoms with positively charged (anodic sites) on the metal surface and the skeleton of inhibitor compound cover the cathodic sites this action form thin layer adsorbed on the metal surface to prevent the corrosion processes. The present of benzene ring, which has electrons density of π-bonding that enhancement the adsorption process and gives the very good inhibition efficiency. Another away the adsorption can be occurs due to the adsorbed an anion on the positive charge on C – steel surface. The SEM image of C-steel that immersion one day in

corrosive medium with the optimization concentration of Gliclazide drug (10 x 10^{-5}M) confirm formation thin layer adsorbed on the metal surface and prevent the corrosion processes, **Figure 17**.

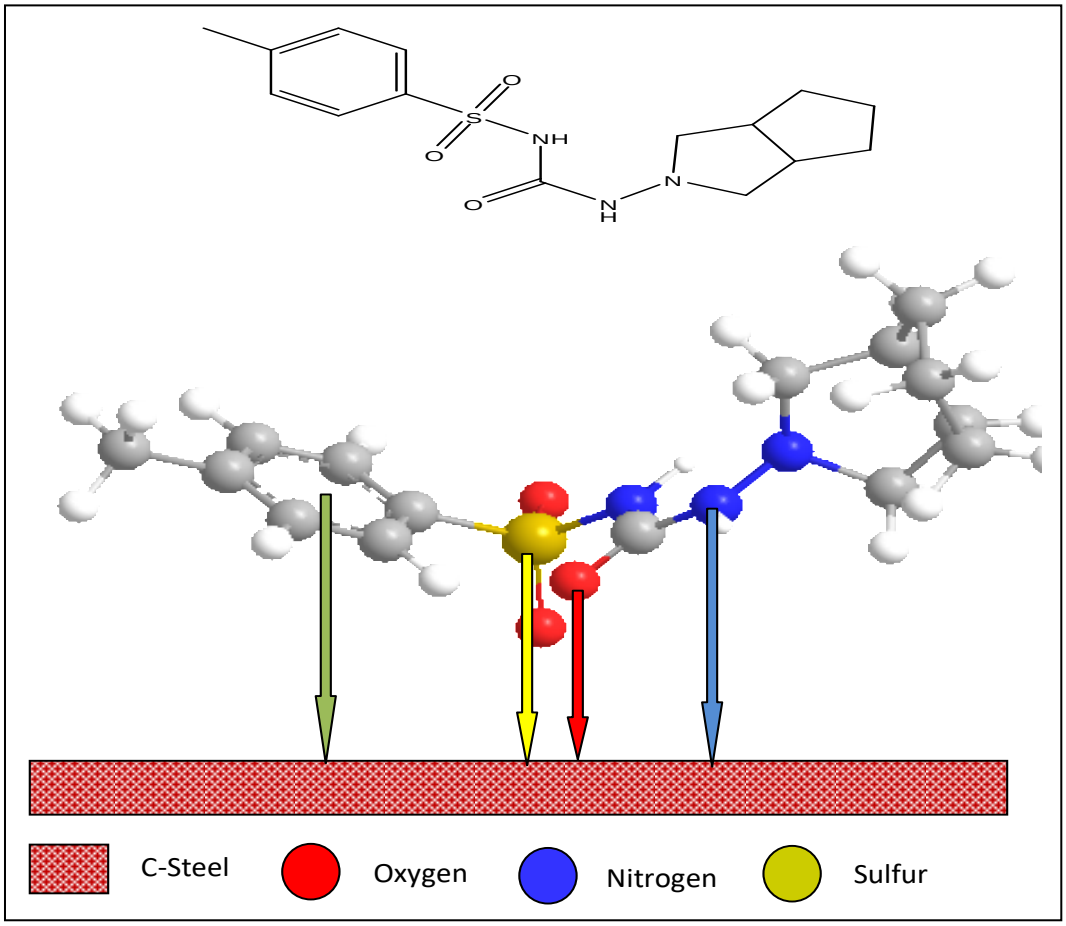

Figure 16: Schema model illustrated the adsorption of gliclazide structure on the C – steel surface.

This meaning, the gliclazide molecule attached with anodic site and covered somewhat of cathodic area, so that the corrosion rate in presence of gliclazide is anodic-cathodic control.

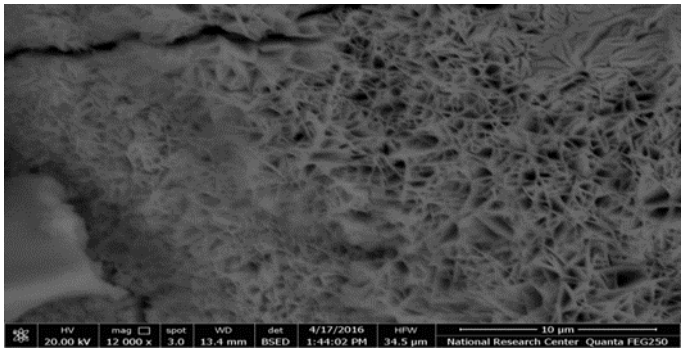

Figure 17: SEM image of C-steel that immersed in the corrosive medium with 10 x10^{-5}M gliclazide drug one day.

4. Conclusion

- By comparison the results with Pourbaix Atlas E-PH diagram clarify that:

(i) The dissolved corrosion product in H_2SO_4 media is Fe SO_4.

(ii) The undissolved corrosion product in H_2SO_4 media is Fe O.

(iii)The corrosion processes in ethanol media are set up at (pH= 6.8) i.e. second passivity region.

- The collective ethanol molecules are not only adsorbed on the electron sink area, but also covered the electron source area too.
- The area of electron source (cathodic area) decreased by heat treatment regime be side increasing of electron sink (anodic area).
- The polarization affected the donor functional groups of glcolazide molecules and oriented them to the electron sink area on the electrode surface and slow dawn the dissolution of metal.
- The moderate size of Glcolazide molecules allow to cover somewhat area of electron source, so that both the metal dissolution and the hydrogen evolution.
- The polarization process affects the orientation and adsorption of the inhibitor molecules.
- By applied Evans diagram principle Glcolazide classified as anodic – cathodic inhibitor, where it adsorbed on anodic sites and covered some of neighbor cathodic sites.

References

[1] Raspini, I. A. Influence of Sodium Salts of Organic Acids as Additives on Localized Corrosion of Aluminum and Its Alloys, *Corrosion*, 1993, 49:821-828.

[2] Migahed, M.A.; Azzam, E. M. S.; Al-Sabagh, A. M. Corrosion inhibition of mild steel in 1 M sulfuric acid solution using anionic surfactant, *Mater. Chem. Phys*., 2004, 85:273-279.

[3] Villamil, R. F.V.; Corio, P.; Rubim, J. C.; Siliva, M. L. Effect of sodium dodecylsulfate on copper corrosion in sulfuric acid media in the absence and presence of benzotriazole, *J. Electroanal. Chem.* 1999, 472:112-119.

[4] Abd El Rehim, S. S.; Hassan, H.; Amin, M. A. The corrosion inhibition study of sodium dodecyl benzene sulphonate to aluminum and its alloys in 1.0 M HCl solution, *Mater. Chem. Phys.* 2003, 78:337-348.

[5] Guo, R.; Liu, T.; Wei, X. Effects of SDS and some alcohols on the inhibition efficiency of corrosion for nickel, *Colloids Surf., A*, 2002, 209:37-45.

[6] Branzoi, V.; Golgovici, F.; Branzoi, F. Aluminum corrosion in hydrochloric acid solutions and the effect of some organic inhibitors, *Mater. Chem. Phys*. 2002, 78: 122-131.

[7] Elachouri, M.; Hajji, M. S.; Salem, M.; Kertit, S.; Aride, J.; Coudert, R.; Essassi, E. Some Nonionic Surfactants as Inhibitors of the Corrosion of Iron in Acid Chloride Solutions, *Corrosion*, 1996, 52:103-108.

[8] Algaber, A. S.; El-Nemma, E. M.; Saleh, M. M. Effect of octylphenol polyethylene oxide on the corrosion inhibition of steel in 0.5 M H_2SO_4, *Mater. Chem. Phys*. 2004, 86:26-32.

[9] Fouda, A. S; El-Ewady, G.; Ali, Adel H. Corrosion Protection of Carbon Steel by using Simvastatin Drug in HCl Medium, *Journal of Applicable Chemistry*, 2017, 6 (5):701-718.

[10] Fouda, A. S. ; Ali, Adel H. Egy- dronate drug as promising corrosion inhibitor of C - steel in aqueous medium, *Zastita Materijala*, 2018, 59 (1):126 - 140

[11] Narayan, R. *An Introduction to Metallic Corrosion and its Prevention*, Oxford, New Delhi, 1983, p73.

[12] Ailor, W. H. *Handbook of Corrosion Testing and Evaluation*, John Wiley &Sons, Inc., New York, 1971, p173-174.

[13] Dacres, Sutula C. M.; Larrick, B. F. A Comparison of Procedures Used in Assessing the Anodic Corrosion of Metal Matrix Composites and Lead Alloys for Use in Lead-Acid Batteries, *Electrochem. Soc.*, 1983, 130: 981-985.

[14] Crow, D. R. *Principles and Applications of Electrochemistry*, Chapman and Hall, London, 3rd ed. 1988.

[15] Pourbaix, M. *Atlas of Electrochemical Equilibria, In Aqueous Solutions*, Pergamon Press, Oxford 1966.

[16] Fouda, A. S.; El-Ewady, G. and Ali, A. H. Modazar as promising corrosion inhibitor of carbon steel in hydrochloric acid solution; *Green Chemistry Letters and Reviews*, 2017,10 (2):88-100.

[17] Fouda, A. S.; El-Ewady, G.; Ali, Adel H. Corrosion Inhibition of Carbon Steel in hydrochloric acid medium using Gliclazide drug, *Journal for Electrochemistry and Plating Technology*, November, 2017, 1 :1-20.

[18] Selim, S. R. Review Research to Professor Degree, Interpretation Part Laboratory of Faculty of Science, Al-Azher University, 2002: p50.

[19] Solmaz, R.; Kardas, G., Tazc, B.; Erbil, M. Adsorption and corrosion inhibitive properties of 2-amino-5-mercapto-1, 3, 4-thiadiazole on mild steel in hydrochloric acid media, *colloids. Surf. A, physicochem. Eng. Aspects*, 2008, 312: 7-17.

[20] Wahdan, M. H.; Hermas, A. A.; Morad, M. S. Corrosion inhibition of carbon-steels by propargyltriphenylphosphonium bromide in H_2SO_4 solution, *Mater. Chem. Phys*. 2002, 76: 111-118.

[21] Bentiss, F.; Trainel, M.; Gengembre, L.; Lagrene, M. A new triazole derivative as inhibitor of the

acid corrosion of mild steel: electrochemical studies, weight loss determination, SEM and XPS, *Appl. Surf. Sci.* 1999, 152:237-249.